NUMERICAL SIMULATIONS OF SUPERCRITICAL INJECTION OF CO_2 IN DUNAJOVICE SANDSTONE

Frédéric Wertz[1], Veronika Vrbová[2,3], Václava Havlová[2]

[1]CVŘ, [2]UJV, [3]VŠCHT, frederic.wertz@cvrez.cz

CO_2 storage is a promising technology to enable further use of coal resources without CO_2 emissions damaging climate. In the Czech Republic, The Dunajovice Sandstone reservoir has been identified as an example of a typical structure suitable for potential geological storage of CO_2 in the Carpathian Foredeep area, and served as a pattern for modelling and simulation purposes in this project. Once injected, CO_2 propagates in its supercritical form and partially dissolves into groundwater. This process acidifies brine and triggers geochemical reactions with the injection wellbore cement, the host rock, as well as the cap rock. These reactions must be quantified and assessed to ensure the security and sustainability of the storage. Here we use the geochemical codes TOUGH2 and TOUGHREACT to estimate the plume propagation as well as the geochemical effects of CO_2 underground injection. Results show a good compatibility of hydrogeological parameters with a 30 years high-rate CO_2 injection, which must be confirmed experimentally. We also notice geochemical stability of sandstone and clay, while the cement is subject to huge mineral transformation. The mechanical structure and tightness of such transformed cement should then be assessed.

Keywords: CO_2 Injection, Plume underground evolution, geochemical evolution

Received 17. 11. 2014, accepted 12. 12. 2014

1. Introduction

CO_2 Capture and Storage (CCS) has been identified as one of the technologies that could achieve 19 % of worldwide CO_2 emissions reduction by 2050 [1]. Indeed, it has the advantage to be potentially plugged into existing infrastructure such as coal power plants, steel and cement factories, oil refineries. Thus business models are not disrupted and Industrials are supporting it, provided the CO_2 price incentive is high enough. Though the technology is not yet widely spread, some pilot projects such as Sleipner in the North Sea [2] have been already existing, simulated and monitored for more than 15 years. This has allowed the development on new monitoring techniques and modelling tools that could be efficiently benchmarked with reality. Though CCS deployment still faces numerous technological challenges from the capture side, injection and storage of CO_2 involve long-term risks assessment and require a good knowledge of the underground site, its geology, hydrogeology and geochemistry.

Long-term safety of a CO_2 storage project itself depends on the stability of the reservoir and on a proper assessment of CO_2 leakage and fluid displacement [2, 3]. Three components are particularly concerned by CO_2 injection: wellbore, host rock and cap rock. First, cap rock tightness must be monitored and ensured during the entire lifetime of the CCS project to avoid potential diffuse leakages. Once in the host rock, CO_2-induced geochemical reactions must not clog its porosity, which would result in lower injectivity. Finally, the most critical leakage potential comes from the wellbore itself and can take various forms [4]: between casing and cement, through the cement pore space, through fractures in the cement, and between cement and rock. To avoid these risks and especially cement fracturing, the wellbore mechanical integrity must be ensured. Indeed, huge geochemical changes may occur when basic materials (cement) are in contact with CO_2-acidified brine [5].

That is why this Research Project aims at analysing in laboratory different mineral evolution of rocks exposed to CO_2-acidified brine. To complement and reproduce these experiments, numerical simulations are done in parallel. This allows better understanding and interpretation of different occurring processes. Hydrogeological simulations with TOUGH2 [6] are done to upscale in space (up to 10 km), and time (up to 300 years) the CO_2 plume propagation (1 Mt_{CO2}/year injected during 30 years), while geochemical simulations with TOUGHREACT [7] are conducted to upscale in time the observed geochemical reactions.

The aim of this numerical study is to interpret physical and geochemical processes in the underground material occurring within a potential CO_2 storage project in the South-East of the Czech Republic. Namely, we look at the underground extension of the CO_2 plume, as well as the geochemical evolution of the three media in contact with CO_2: cement, host rock and cap rock. An important indicator of the system evolution is the porosity of each of the media. Indeed, higher porosity in the cap rock may induce higher permeability, which is a risk of diffuse leakage. On the other hand, lower porosity in the reservoir may induce lower injectivity and near-well pressure build-up. This is a risk that may lead to mechanical cracks in the cement or cap rock. Also, clogging cement porosity may create pressure build-up at the pore scale and lead to local micro-cracks.

2. Physicochemical Background

2.1. Hydrogeological situation

The Dunajovice Sandstone already hosts a seasonal natural gas storage facility [8]. This is a proof of quite suitable hydrogeological parameters to conduct CO_2 injection in similar geological structures in the area. Assuming that these physical parameters extend up to the potential injection location, we can then reuse the data (see Tab. 1) in the injection model. Permeability in horizontal direction κ_R is usually higher than the one in the vertical direction κ_Z because of the sedimentation processes. Also, the reservoir contains shale lens that reduce yet allow vertical communication. We here use a factor 100 between κ_R and κ_Z to account for that. CO2 properties (density and viscosity) are dynamically determined by TOUGH2 thermodynamic module ECO2N [9] as a function of Pressure P, Temperature T and Salinity S.

Tab. 1 Hydrogeological parameters

Parameter	Sandstone
Thickness	36 m
Porosity	18%
Permeability κ_R	450 mD
Permeability κ_Z	4.5 mD
Pressure P	81 bar
Temperature T	35°C
Salinity S	68 g/L
CO_2 density	f(P,T,S) [9]
CO_2 viscosity	f(P,T,S) [9]

2.2. Solutions composition

Tab. 2 Brine composition [mg/L]

Element	Brine	Acidified Brine
T	35°C	35°C
pH	7.65	***4.78***
Ca^{2+}	12.1	12.1
Mg^{2+}	1850.9	1850.9
Na^{+}	19298.4	19298.4
K^{+}	960.1	960.1
Li^{+}	50.0	50.0
Cl^{-}	34572.0	34572.0
CO_2	3094.7	***75741***
SO_4^{2-}	120.5	120.5
NH_4^{+}	77.0	77.0

Some brine samples were taken and chemically analysed for the purpose of the project. Then an artificial brine composition was reconstituted. For collateral batch experiments [10], the brine is in contact with supercritical CO_2 at 81 bar and 35°C. CO_2 then dissolves into the brine up to the thermodynamic equilibrium. This process acidifies the brine and enriches it by carbonate ions, according to:

$$CO_{2g} \leftrightarrow CO_{2aq} \qquad CO_{2aq} + H_2O \leftrightarrow H_2CO_3 \qquad (1)$$

$$H_2CO_3 \leftrightarrow HCO_3^- + H^+ \qquad HCO_3^- \leftrightarrow CO_3^{2-} + H^+$$

This acidified brine is then used both in experiments and simulations. Tab. 2 gives its composition.

2.3. Solid phases composition

The host rock (Dunajovice Sandstone) was sampled and analysed in order to determine its mineral composition. Tab. 3 summarises the main minerals constituting sandstone

Tab. 3 Sandstone composition

Mineral	%Vol)
Quartz	56.8
Muscovite	21.4
Kaolinite	9.9
Microcline	8.2
Chamosite	2.6
Calcite	1.1

The envisaged cement for the wellbore is a normal Portland CEM II/B-M (S-V) 32,5 R. XRF analysis estimates its initial oxides composition (see Tab. 4).

Tab. 4 Cement powder composition (XRF analysis)

Oxide	%Mass
MgO	2.56
Al_2O_3	5.77
SiO_2	19.95
SO_3	3.74
CaO	63.34
Fe_2O_3	2.64

Once hydrated, cement forms minerals and gels, whose composition depends on temperature and initial oxides composition. Tab. 5 gives the final computed mineral composition, assuming an ideal homogeneous hydration (no remaining oxides crystals). Main cement component is then a Ca-Si hydrate (CSH1.6).

Tab. 5 Cement composition

Mineral	Formula	%Vol
CSH1.6	$Ca_{1.6}SiO_{3.6}$:2.58H_2O	42.3
Portlandite	$Ca(OH)_2$	25.2
Ettringite	$Ca_6Al_2(SO_4)_3(OH)_{12}$:26$H_2O$	18.2
Hydrotalcite	$Mg_4Al_2O_7$:10H_2O	5.9
Katoite-Si	$Ca_3Al_2SiO_4(OH)_8$	5.7
Ferrihydrite	$Fe(OH)_3$	1.9

3. Modelling Approach

3.1. Grid and Geometry

For the need of the large-scale hydrogeological simulation, we considered a cylinder (R-Z coordinates) and created a mesh representing the host rock. It is composed of 808 cells with exponentially growing radii. This gives enough precision in the near well zone, while allowing a wide extension of the domain at reduced CPU-cost. Thus Neumann boundary conditions (initial pressure gradient imposed) are far enough from the studied subject.. Thickness is reduced in the top layers to better account for the upward widening of the plume due to buoyancy (Fig. 1).

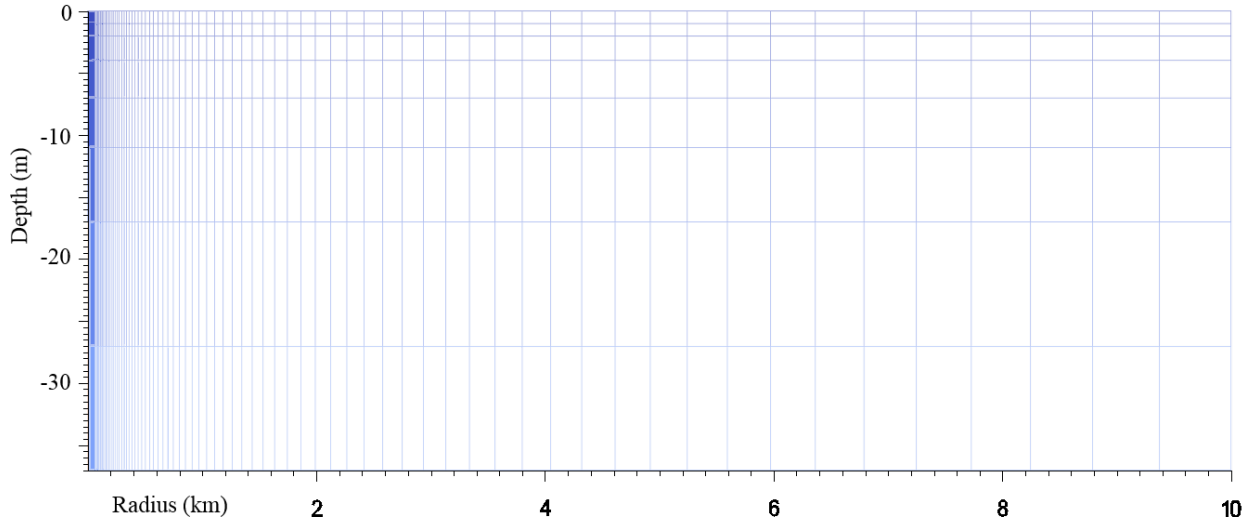

Fig. 1 808 cells grid, 36 m high, 10 km wide with exponential cell size, R-Z geometry

3.2. Two-phase flow and Darcy law

Hydrogeological simulations are needed to estimate CO_2 plume propagation. TOUGH2 code [6] is used and assumes the host rock is a homogeneous porous medium. Thus, Darcy law best describes the fluids flow through a porous cell for each dimension according to:

$$q_V = \frac{\kappa \cdot \kappa_r}{\mu} \cdot \left(\frac{\Delta P}{\varepsilon} + \Delta\rho \cdot g \right) \quad (2)$$

where q_v is the volumetric fluid flux, κ the intrinsic Permeability of the porous material, κ_r its relative permeability model, μ the fluid viscosity, ΔP the overpressure between the 2 boundaries of the cell, ε the cell thickness, $\Delta\rho$ the density difference between the gas and the brine, g the gravity. Relative permeabilities κ_r (or k_r) are determined according van Genuchten model [11] and parameters (Tab. 6):

$$k_{rl} = \begin{cases} \sqrt{S^*}\left\{1-\left(1-[S^*]^{1/\lambda}\right)^{\lambda}\right\}^2 & \text{if } S_l < S_{ls} \\ 1 & \text{if } S_l \geq S_{ls} \end{cases} \quad (3)$$

$$k_{rg} = \begin{cases} 1-k_{rl} & \text{if } S_{gr}=0 \\ \left(1-\hat{S}\right)^2\left(1-\hat{S}^2\right) & \text{if } S_{gr}>0 \end{cases} \quad (4)$$

where $S^* = (S_l-S_{lr})/(S_{ls}-S_{lr})$, with S_l the liquid saturation, and $\hat{S} = (S_l-S_{lr})/(1-S_{lr}-S_{gr})$. k_{rl} stands for the relative permeability of the liquid phase, while k_{rg} stands for the relative permeability of the gaseous phase. Similarly, Capillary pressure is also computed by van Genuchten function:

$$P_{cap} = -P_0\left([S^*]^{-1/\lambda}-1\right)^{1-\lambda} \quad (5)$$

Tab. 6 Van Genuchten parameters

Parameter	Sandstone
λ	0.457
S_{lr}	0.3
S_{ls}	1
S_{gr}	0.05
$1/P_0$	1 Pa^{-1}
P_{max}	1E7 Pa

3.3. Geochemical parameters

Geochemical analyses are done thanks to batch simulations. Thermodynamic equilibrium, elements speciation, and mineral saturation indexes are determined using Thermoddem database [12]. When not at the thermodynamic equilibrium, minerals tend to precipitate (if over-saturated) or dissolve (if under-saturated). But their internal structure leads to heterogeneous kinetic rates. TOUGHREACT [7] computes the rate law for mineral dissolution and precipitation according to Lasaga formalism [13]:

$$r_n = \pm k A_n \left|1-\Omega_n^{\theta}\right|^{\eta} \quad (6)$$

A positive value for r_n (mol s^{-1}) corresponds to dissolution of the mineral n (negative for precipitation), k is the rate constant (mol m^{-2} s^{-1}) depending on the tem-

perature, A_n is the specific reactive surface area ($m^2.kg_w^{-1}$), and Ω_n is the saturation ratio of the mineral n (ratio between the activity product and the equilibrium constant). The empirical parameters θ and η are determined from experiments, otherwise they are usually taken as 1. The dependence of the rate constant k with temperature is calculated by means of the Arrhenius equation [13]:

$$k = k_{25} \exp\left[\frac{-E_a}{R}\left(\frac{1}{T} - \frac{1}{298.15}\right)\right] \quad (7)$$

where E_a ($J.mol^{-1}$) is the activation energy, k_{25} ($mol.m^{-2}.s^{-1}$) the rate constant at 25 °C, R ($J.K^{-1}.mol^{-1}$) is the universal gas constant and T (K) the absolute temperature. Mineral precipitation and dissolution rates can be influenced by different mechanisms, for example acid or carbonate mechanisms [14].

$$\begin{aligned} k = {} & k_{25}^{nu} \exp\left[\frac{-E_a^{nu}}{R}\left(\frac{1}{T} - \frac{1}{298.15}\right)\right] \\ & + k_{25}^{H} \exp\left[\frac{-E_a^{H}}{R}\left(\frac{1}{T} - \frac{1}{298.15}\right)\right] a_H^{nH} \\ & + k_{25}^{CO2} \exp\left[\frac{-E_a^{CO2}}{R}\left(\frac{1}{T} - \frac{1}{298.15}\right)\right] a_{CO2,aq}^{nCO2} \end{aligned} \quad (8)$$

where superscripts or subscripts *nu*, *H* and *CO2* indicate neutral, acid and carbonate mechanisms, respectively, and *a* is the activity of the corresponding species. Tab. 7 summarizes the different kinetic parameters further used in the simulations.

Tab. 7 Kinetic coefficients [14, 15, 16, 17]

Mineral	k25 mol/m²/s	EA kJ/mol	n	A m²/g
Portlandite	2.18E-8	74.9		0.154
acid mech.	8.04E-4	74.9	0.6	
CSH1.6	1.6E-18			2.0
acid mech.	5.94E-8		0.275	
Katoite	1.6E-18			0.057
acid mech.	5.94E-8		0.275	
Hydrotalcite	1.6E-18			0.1
acid mech.	5.94E-8		0.275	
Ettringite	1.14E-12			0.098
Calcite	1.55E-6	23.5		0.026
acid mech.	5.0E-1	14.4		
carb mech.	6.58E-3	56.1		
Magnesite	4.47E-10	63		0.026
acid mech.	4.37E-5	19		
Dolomite	1.05E-8	30.8		0.0012
acid mech	2.85E-4	45.9	0.615	

k25 is the kinetic constant at 25°C, EA the activation energy, n the degree of the additional mechanism (H^+ or HCO_3^-), A the reactive surface of the material

4. Results and Discussion

4.1. CO_2 Plume Propagation

When injecting CO_2 at the high rate of 1 Mt/year in a 100% water saturated pore space, we first notice a near well pressure build-up (Fig. 3) of ΔP being 23 bar. This is necessary so that injected CO_2 creates pathways for further diffusion in the porous medium. This may induce mechanical cracks to the cap rock and endanger its tightness. However, this local and temporarily effect can be overcome by slower injection during the first years if the overall industrial project is compatible.

Then, the near well pressure decreases while pressure builds up in the rest of the reservoir (Fig. 3). This accompanies the formation of the CO_2 plume in the reservoir. Over time, from cylindrical shape, the plume widens its upper body, blocked under the cap rock. After 30 years injection, the near-well overpressure does not exceed 10 bar, while CO_2 plume extension does not exceed 7 km (3.5 km radius) in its wider extent.

However, this situation concerns an ideal case where the cap rock is perfectly plane and horizontal. In case of even a minor slope, CO_2 would spread more in the upward direction. This would trigger a higher plume extent, as well as a higher dissolution rate in unsaturated brine and would accelerate the final CO_2 immobilization. Future simulations require advanced geological assessment in order to better model the underground structure.

After the 30 years injection period, we model further 300 years relaxation time for the system. During this timescale, pressure rapidly recovers its initial gradient, while CO_2 plume further extents due to buoyancy. By reaching new unsaturated brine, CO_2 continues to dissolve. CO_2 dissolution into brine is almost instantaneous, so aqueous CO_2 is at its themodynamic equilibrium of $39g_{CO2}/kg_{brine}$ in each zone hosting or having hosted supercritical CO_2 (Fig. 4).

After 300 years of post-injection relaxation period, CO_2 plume extents to 12 km (6 km radius). The fraction of CO_2 that has dissolved represents 30% of the initial injected CO_2 (Fig. 7). This aqueous CO_2 is much less mobile than supercritical CO_2 that is still in a slow upward motion. We may expect that the intercalation of more permeable and less permeable layers inside the reservoir reduces CO_2 mobility and plume extent.

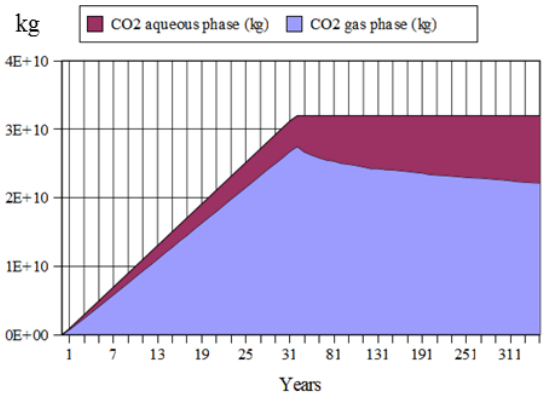

Fig. 2 CO_2 breakdown aqueous/gas (supercritical)

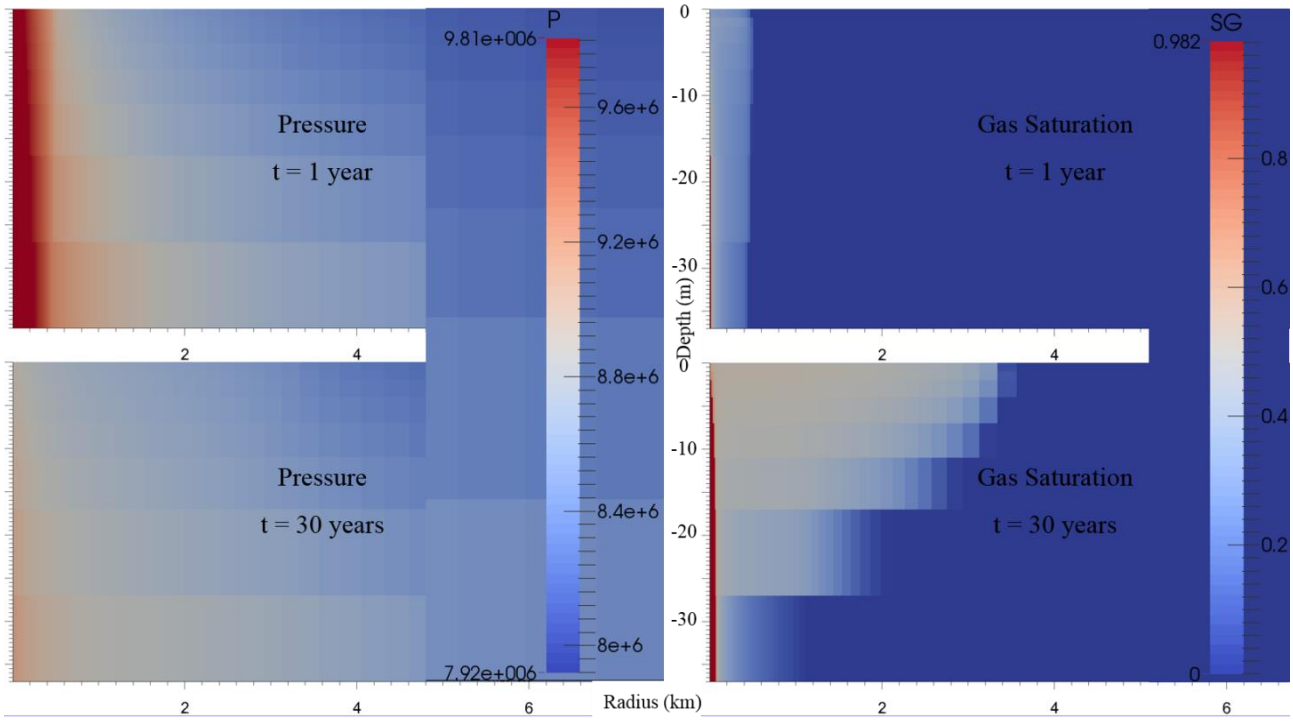

Fig. **3** Pressure (Pa, left) and gas saturation (supercritical CO_2 plume, right), after 1 and 30 years of injection

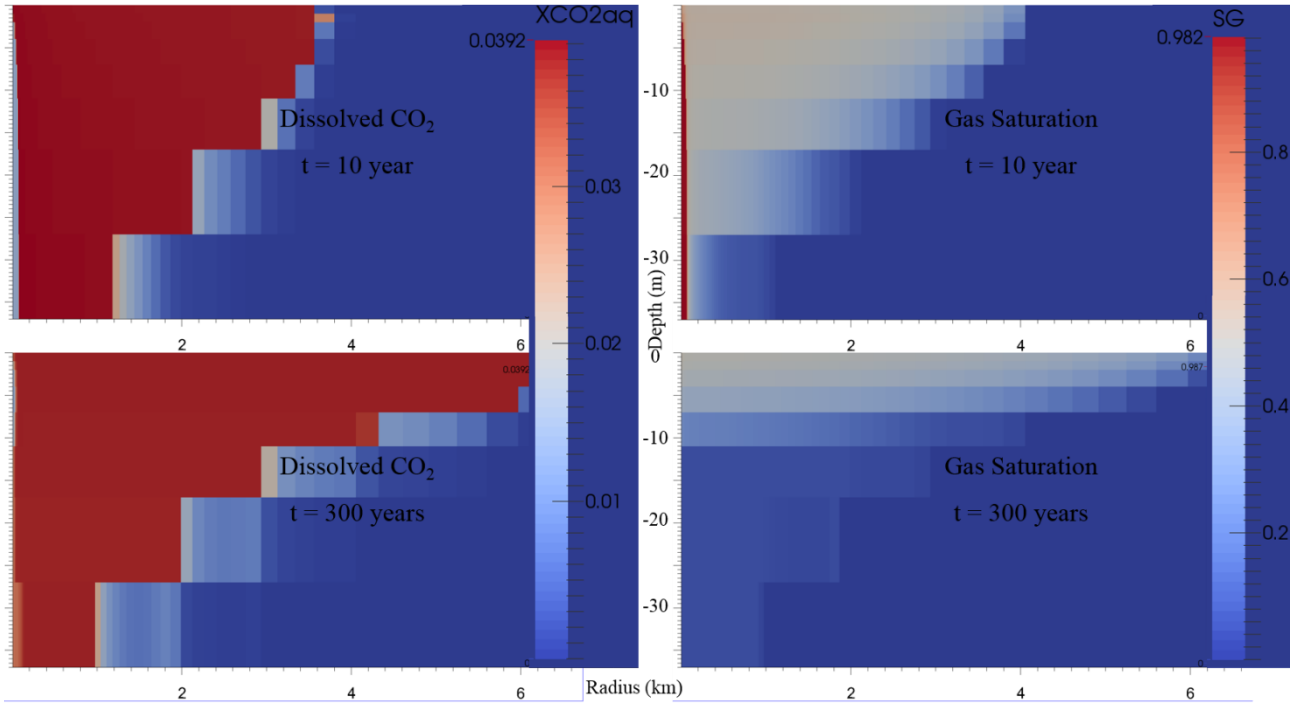

Fig. **4** Dissolved CO_2 (left) and gas saturation (supercritical CO_2 plume, right), 10 and 300 years after injection

4.2. Sandstone geochemical evolution

Batch simulations show a relative stability of sandstone (Fig. 5). This is confirmed by the batch experiment (100 days only). Yet, quartz seems to replace part of the muscovite initially in place. This should be further confirmed, since both components are expected to stay stable, especially after only 100 days of reaction [2].

Since the Mg concentration of the brine is initially high, dissolution of CO_2 into the brine leads to some magnesite precipitation. Overall, the porosity of sandstone is almost unchanged. This decreases the risk of clogging host rock. Thus, permeability is expected to be conserved, which prevents further consequences in terms of cement or cap-rock fracking.

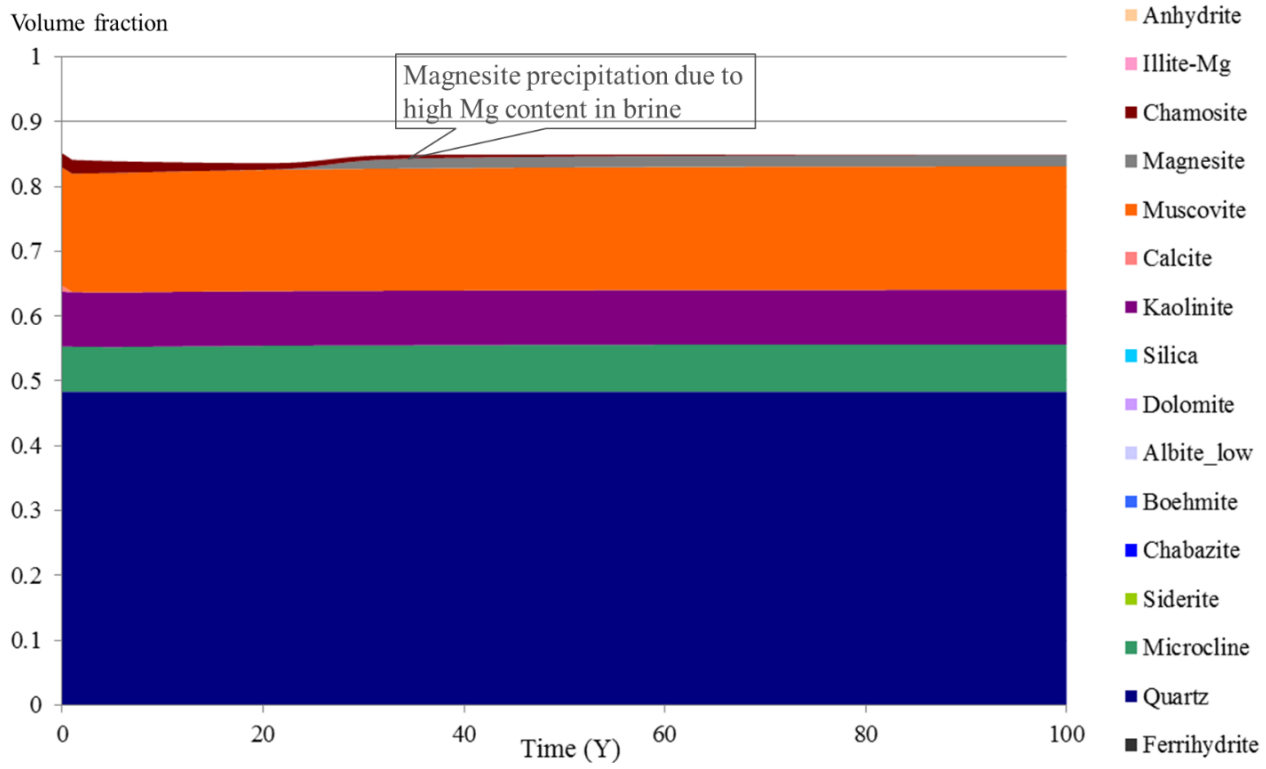

Fig. **5** Sandstone mineral evolution over 100 years

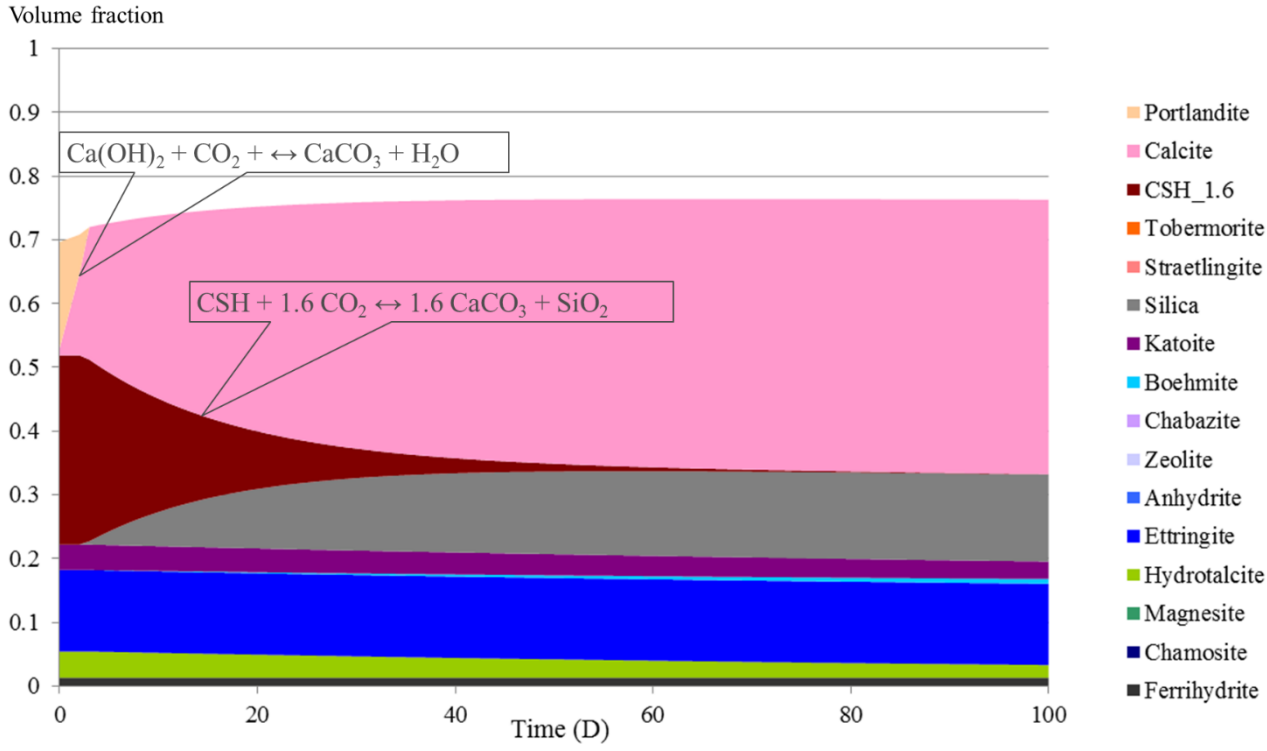

Fig. **6** Portland cement mineral evolution over 100 days

4.3. Cement geochemical evolution

Batch simulation shows dramatic evolution of the cement mineral evolution (Fig. 10). Experiments confirm the fast replacement of portlandite by calcite. Indeed, cement minerals are only stable in basic solutions.

In CO_2-acidified brine, geochemical reactions are inevitable:

$$Ca(OH)_2 + CO_2 + \leftrightarrow CaCO_3 + H_2O \quad (9)$$

Experiments then show a dissolution of ettringite. In the numerical simulation however, ettringite is rather stable, while CSH gel is the next cement component to dissolve and forms calcite and Silica:

$$CSH + 1.6\ CO_2 \leftrightarrow 1.6\ CaCO_3 + SiO_2 \quad (10)$$

This difference might come from the difficulties to characterise cement pastes. Indeed, cement components rather form a solid solution once hydrated. However simulation codes and analysis tools are designed to work with clearly identified mineral phases. Thus, a given composition might be interpreted and treated differently by the two approaches (experiment or simulation). To increase the confidence of the results, better cement-specific thermodynamic databases are required.

Overall, the cement porosity slightly decreases. This is not a danger in itself, however the mineral changes are so huge that mechanical and sealing properties of such cement paste should be further studied. Indeed, the microstructure may not be necessarily homogeneously affected.

5. Conclusion

This study allows to draw preliminary pictures of what a CO_2 storage project in the South-East of the Czech Republic might look like. Given the chosen assumptions, the CO_2 plume is expected to propagate horizontally in the order of several km. Further steps for a potential pilot project in the Czech Republic should include a better characterisation of the geological structural model. In particular, the development of a static geological model (both structures and rock properties) and the subsequent dynamic hydrogeological model would improve the accuracy of future numerical simulations. Indeed, heterogeneous sand layers may lead to faster dissolution and immobilisation of CO_2 in both gaseous and aqueous phases. On the other hand, leaning layers may enable CO_2 plume to propagate faster and further.

Sandstone is expected to be geochemically stable, however, further specific studies should confirm in this particular case. On-going Sleipner project is also based on a saline sandstone aquifer and numerical tools proved remarkably well compared to real monitored data [2]. Thus, we expect a good reliability of the geochemical simulation. Concerning the wellbore, cement paste leaches, which is considered as a normal evolution of cement in underground conditions. However it should be checked whether such leaching could threaten the cement mechanical properties. Otherwise, other pastes and low-pH cement may be considered as well.

Acknowledgement

This study has been co-funded by the Technology Agency of the Czech Republic Project TA03020405 „Development and optimisation of methodologies for research on safety barriers for CO_2 storage as one of the key ways of reduction of GHG content in the atmosphere“ and by the SUSEN Project CZ.1.05/2.1.00/03.0108, realised in the framework of the European Regional Development Fund (ERDF).

References

1. International Energy Agency. Energy Technology perspectives. 2008.
2. Audigane P., Gaus I., Czernichowski-Lauriol I., Pruess K., Xu T. Two-dimensional reactive transport modeling of CO_2 injection in a saline aquifer at the Sleipner site, North Sea. American Journal of Science 2007, 307(7), 974-1008.
3. Pruess K. On CO_2 fluid flow and heat transfer behavior in the subsurface, following leakage from a geologic storage reservoir. Environmental Geology 2008, 54(8), 1677-1686.
4. Gasda S.E., Bachu S., Celia M.A. Spatial characterization of the location of potentially leaky wells penetrating a deep saline aquifer in a mature sedimentary basin. Environmental Geology 2004, 46, 707-720.
5. Wertz F., Gherardi F., Blanc P., Bader A., Fabbri A. Cement CO2-alteration propagation at the well-caprock-reservoir interface and influence of diffusion. International Journal of Greenhouse Gas Control 2013, 12, 9-17.
6. Pruess K., Oldenburg C., Moridis G. TOUGH2 user's guide, Version 2.0. Earth Sciences Division, Lawrence Berkeley National Laboratory University of California, Berkeley, California. Report LBNL-43134, 1999.
7. Xu H., Sonnenthal E.L., Spycher N., Pruess K. TOUGHREACT user's guide: a simulation program for nonisothermal multiphase reactive geochemical transport in variably saturated geologic media. Lawrence Berkeley National Laboratory, Berkeley, California. Report LBNL-55460, 2004.
8. http://members.igu.org/html/wgc2003/WGC_pdffiles/data/Europe/att/UGS_86.html [accessed 10/11/2014]
9. Pruess K. ECO2N: A TOUGH2 Fluid Property Module for Mixtures of Water, NaCl, and CO2. Earth Sciences Division, Lawrence Berkeley National Laboratory University of California, Berkeley, California. Report LBNL-57952, 2005.
10. Havlová V. Průběžná roční zpráva projektu FR-TI1/379 Výzkum a vývoj metod a technologií zachycování CO2 v elektrárnách na fosilní paliva a ukládání do geologických formací v podmínkách ČR. Etapy 3.3, 3.4 a 3.5. ÚJV Řež, a. s., 2012.

11. Van Genuchten M.Th. A Closed-Form Equation for Predicting the Hydraulic Conductivity of Unsaturated Soils, Soil Science Society 1980, 44, 892 – 898.
12. Blanc P., Lassin A., Piantone P., Azaroual M., Jacquemet N., Fabbri A., Gaucher E.C.. Thermoddem: a geochemical database focused on low temperature water/rock interactions and waste materials. Applied Geochemistry 2012, 27 (10), 2107–2116.
13. Lasaga A.C. Rate laws in chemical reactions. In: Lasaga, A.C., Kirkpatrick, R.J. (Eds.), Kinetics of Geochemical Processes. Reviews in Mineralogy 1981, 8, 135–169.
14. Palandri J.L., Kharaka Y.K. A compilation of rate parameters of water–mineral interaction kinetics for application to geochemical modelling. U.S. Geological Survey Report 2004-1068.
15. Galí S., Ayora C., Alfonso P., Tauler E., Labrador M. Kinetics of dolomite–portlandite reaction: Application to portland cement concrete. Cement and Concrete Research 2001, 31 (6), 933-939
16. Schweizer Ch. R. Calciumsilikathydrat-Mineralien. Lösungskinetik und ihr Einfluss auf das Auswaschverhalten von Substanzen aus einer Ablagerung mit Rückständen aus Müllverbrennungsanlagen. PhD thesis, dipl. Chem. Universität Basel, Zürich und Dübendorf, 1999.
17. Baur I., Keller P., Mavrocordatos D., Wehrli B., Johnson C.A. Dissolution–precipitation behaviour of ettringite, mono- sulfate, and calcium silicate hydrate. Cement and Concrete Research 2004, 34 (2), 341–348